

to date. In traditional MALDI, an organic matrix is mixed with the sample on the target plate and irradiated by a ultraviolet or IR light generated by a pulsed and focused laser. The matrix absorbs the light at the wavelength of the laser, leading to a soft desorption/ionization of the intact compounds of interest (Gross, 2004; Karas *et al.*, 1985; Tanaka *et al.*, 1988). Figure 1c illustrates the MALDI mechanism.

3. MALDI IMAGING

By scanning a sample surface with the MALDI matrix/laser setup and registering individual mass spectra for each pixel, a 2D ion density map can be reconstructed using appropriate software. Direct MALDI-IMS analysis of clinical samples offers a unique approach to reveal the spatial expression of biomolecules linked with pathological disease and other clinical information. MALDI imaging is also suitable as a biomarker discovery tool by comparing the relative quantities and/or spatial distribution patterns of molecules in pathological and normal samples. The localization and abundance of biomarkers identified in tissue sections are used to understand disease progression at a molecular level. The main advantages of a direct biomarker analysis using MALDI imaging are that it provides spatial distribution patterns and is free from extraction, purification, or separation steps, hence avoiding procedures that are both time-consuming and jeopardize sample integrity (Chaurand *et al.*, 2006; Hayasaka *et al.*, 2010; Herring *et al.*, 2007; Schwartz *et al.*, 2003; Sugiura *et al.*, 2009). With the currently available imaging software packages, we can construct multiplexed imaging maps of selected biomolecules within tissue sections. The laser energy is used in a raster scan pattern to ionize the molecules, which are present as discrete spots or pixel. For each pixel the full mass spectrum is represented. The data acquisition time for IMS was shortened by the introduction of N₂ (337-nm) or neodymium-doped yttrium aluminum garnet (Nd:YAG) (355-nm) lasers with repetition rates of 200–1000 Hz with pulse lengths of 3 ns. The laser spot size of MALDI-MS is decreased from 100–150 to 20 μm , rendering higher spatial resolution of biomolecules on the tissue surface. Further, a higher spatial resolution can be attained with a MALDI instrument equipped with a highly focused laser. Chaurand *et al.* (2007) used a laser beam at 7 μm , which is in the order of the diameter of a single cell to detect protein ions. However, a decrease in sensitivity is observed while increasing the resolution in this manner. Figure 2 shows an example of MALDI-IMS analysis of protein from tissue section.

In addition to increased sample integrity, the great advantage of IMS is that it allows the construction of numerous ion images of molecules detected in a single run. This technique does not require previous

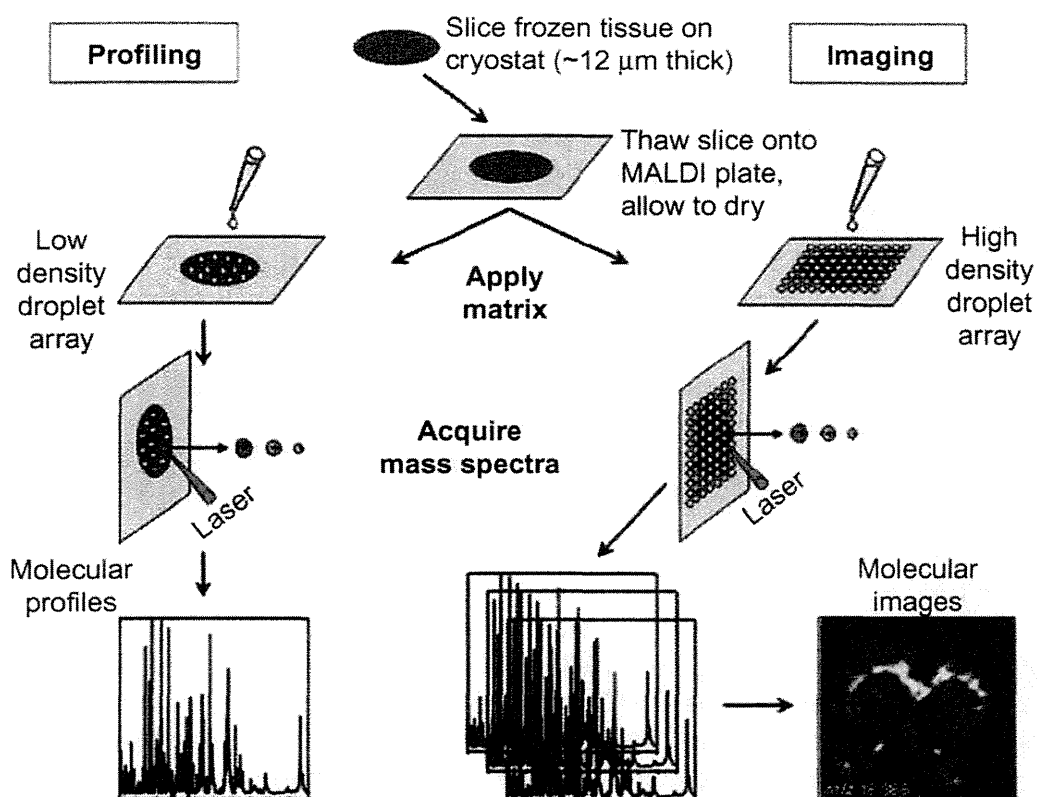


FIGURE 2 Scheme presenting the protein profiling and imaging analytical strategies from thin tissue sections. Reprinted from Chaurand (2006) with permission from American Chemical Society. (See Color Insert.)

labeling with fluorescent probes or radioactive isotopes. MS analyses may be performed for imaging of biomolecules at low concentrations; the detection of 500 attomol has been reported in a single cell (Northen *et al.*, 2007). Another advantage when using MS is the specific identification of molecules; tandem MS is used to identify compounds for which no previous knowledge is required. For this, two MS analyzers are used: one for the selection of the ion of interest before fragmentation, and the second is used for the analysis of fragmented masses. Thus the use of MS is rapid, sensitive, and free from complicated sample procedures for the analysis of unknown biological tissue samples.

3.1. Sample Handling

Sampling handling is a very important concern for imaging and identification of biomolecules in tissue samples. Consideration must be given to the storage of the tissue sample after surgical removal from the human or animal body to prevent *ex vivo* degradation and alteration processes. The sectioning, washing, and staining of tissue, the choice of matrix, and its application on the tissue section are other parameters to optimize in order to obtain better-quality data.

3.1.1. Storage of Samples

Tissue storage is the most important part of the protocol for IMS studies to maintain the integrity of both the molecular composition and the spatial localization of analytes. When sampling is performed through surgical removal of tissue, molecular processes such as protein degradation continue in the *ex vivo* state. These processes should be halted immediately, either through freezing in liquid nitrogen or heat stabilization (Schwartz *et al.*, 2003). Chaurand *et al.* (2008) reported a long preservation method of tissue samples with ethanol for generating high-quality histological sections that enable high-quality images of biomolecules in tissue sample. Previously archived samples, on the other hand, are often fixed with paraformaldehyde and embedded in paraffin. Due to the cross-linking between molecules caused by this preservation method, special methods for specific tissue digestion have been developed (Wisztorski *et al.*, 2010).

3.1.2. Sectioning of Tissue

The next important part of imaging experiments is the sectioning of tissue sample into thin slices and the subsequent mounting of these tissue slices onto an appropriate target. Before tissue sectioning, the frozen tissue samples are transferred from the -80°C freezer to the cryostat chamber at -20°C for 30 minutes to thermally equilibrate the tissue. The tissue is usually embedded on an optimal cutting temperature (OCT) polymer, which supports easy handling and precise microtoming of sections. However, the use of OCT compounds causes a suppression of MALDI analyte signals in MS and should, if possible, be avoided (Schwartz *et al.*, 2003). Figure 3 shows the mass spectra of rat liver with suppression of MALDI-MS signals when OCT is used as a supporting material.

The use of gelatin is an alternative method for embedding the tissue sample where the mass spectrum is free from background signals compared with the use of OCT (Chen *et al.*, 2009). The embedded tissue is fixed on a sample stage and the temperature is maintained between 5°C and -25°C . The optimal temperature is set depending on the type of tissue to be analyzed and is followed by slicing of tissue with a steel microtome blade. For MALDI-IMS, the tissue sections are usually 5–20- μm thick (Chaurand *et al.*, 2006; Schwartz *et al.*, 2003).

The next step is the proper transfer of the sliced tissue section onto an electrically conductive steel plate or a glass slide. Thicker sections of tissue are more suitable when transferring them to the target plate because thinner sections break more easily. The first method of tissue transfer is performed by simply placing the plate in the cryostat chamber kept at -15°C while sectioning. An artist's brush is used to pick up the tissue section and gently place it on the cold plate, followed by gentle warming

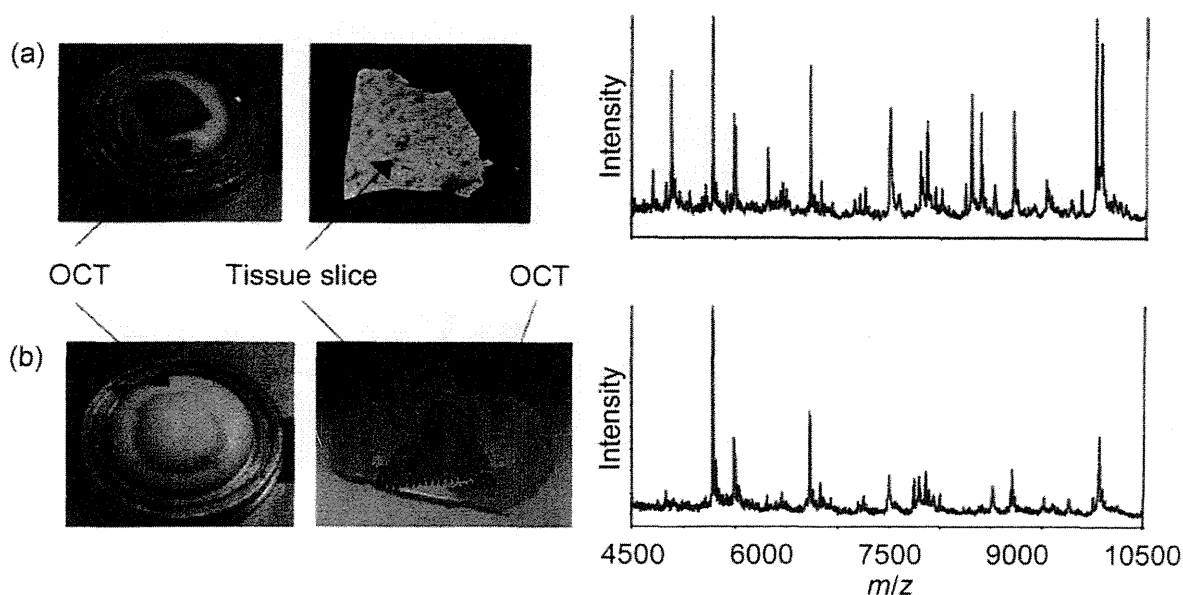


FIGURE 3 Effect of optimal cutting temperature (OCT) on MALDI signal from rat liver. (a) Optimal procedure where OCT is used to adhere the tissue to the sample stage but does not come into contact with the sliced tissue. The resulting spectrum shows many intense signals between m/z 4500 and 10500. (b) The tissue was embedded in OCT and attached to the sample stage. The resulting tissue slice is surrounded by OCT on the MALDI plate, and the resulting spectrum contains only about half of the signals as in (a). Reprinted from Schwartz *et al.* (2003) with permission from John Wiley and Sons.

of the plate by touching the backside of the plate with a fingertip. The tissue is thereby thaw-mounted on the target plate. In the second method, the plate is kept at room temperature and placed over the sliced frozen section, and the tissue is thereby simply thawed on the target plate. Great care should be taken with both methods to retain the shape of the tissue. Obviously, folding or stretching caused during the sectioning of tissue section may affect the molecule distribution analysis and prevents detection of some of the molecules from the tissue surface.

3.1.3. Washing Tissue Sections

A tissue sample is generally washed to remove contaminants such as tissue-embedding media as well as lipids or biological salts that may affect the profiling and identification of peptides and proteins in MALDI-MS analysis. Washing a tissue section with 70% ethanol can remove salts, followed by a 90%–100% ethanol wash to dehydrate and fixate the tissue (Lemaire *et al.* 2006b; Schwartz *et al.*, 2003). Lemaire *et al.* demonstrated a procedure for washing a tissue section with five different organic solvents (chloroform, xylene, toluene, hexane, and acetone) for the identification of proteins in tissue samples and repeated the procedure with fresh solvents. The detection of protein signals is increased when the tissue

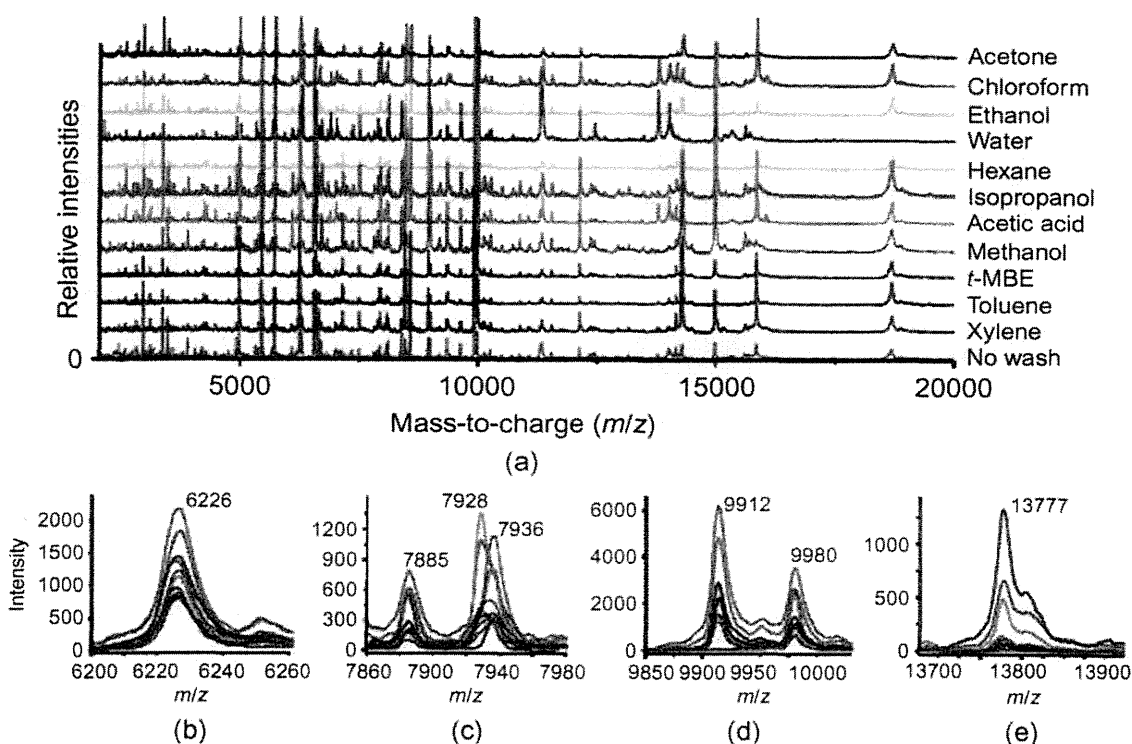


FIGURE 4 Average MALDI-IMS protein profiles directly acquired from serial mouse liver tissue sections not washed or washed with different solvent systems. (a) Full mass range; (b)–(e) selected mass signals showing specific behaviors for the different washes. Reprinted from Seeley *et al.* (2008) with permission from Springer. (See Color Insert.)

sections are washed with organic solvent compared with untreated samples (Lemaire *et al.*, 2006b). Seeley *et al.* (2008) reported a new washing procedure to enhance protein detection in terms of both the number of observed peaks and the signal intensity. They demonstrated that the use of 12 different washing solvents established the most effective condition for direct protein analysis from the surface of tissue section. They also obtained a high detection sensitivity of protein signals, matrix crystal formations, and histological integrity of the tissues by washing with 70% isopropanol for 30 seconds followed by a 90% isopropanol wash for 30 seconds. Figure 4 shows the MALDI-IMS results for protein detection in mouse liver tissue sections after washing with different organic solvents.

3.1.4. Histological Staining of the Section

Histological staining of the tissue section is necessary to interpret the ion images obtained from the IMS results with the tissue section used in the experiments. The optical image obtained by the microscope is also used to superimpose the images acquired by IMS analysis to see the localization of molecules in tissue section. Hematoxylin-eosin (H&E) staining is a very popular histological method for MALDI-IMS results (Walch *et al.*, 2008). In IMS, two serial sections are sliced from tissue; one is used for imaging

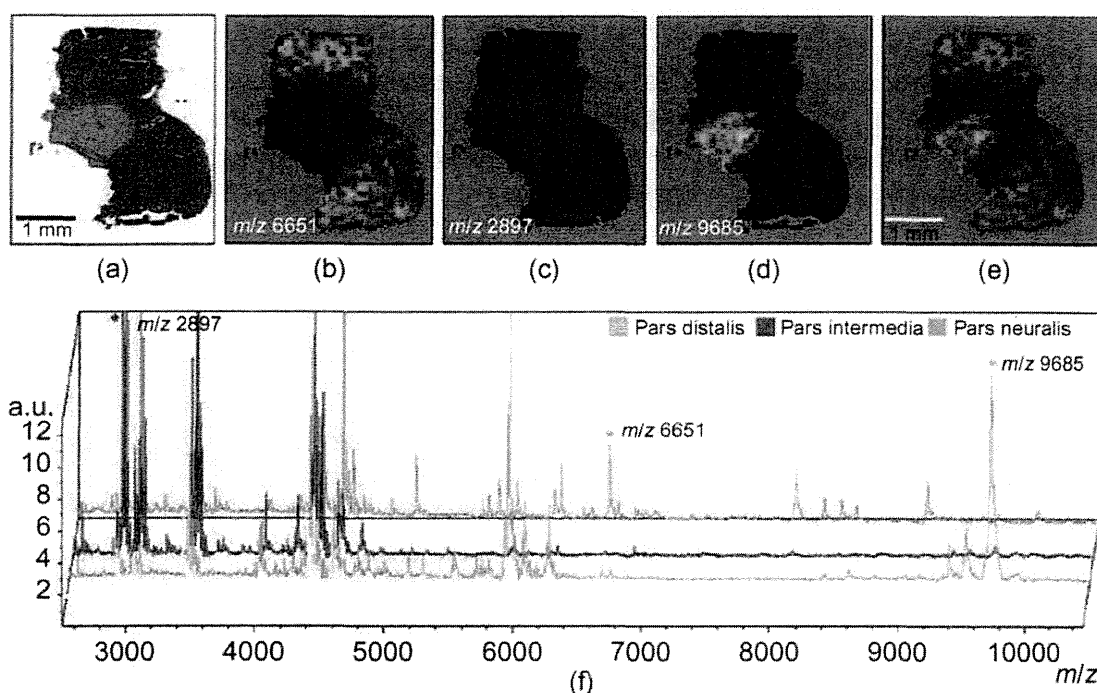


FIGURE 5 MALDI-IMS of a tissue section of rat pituitary gland. (a) Optical microscopic image of an H&E-stained tissues section. The staining was done after the MALDI measurement of the tissue section. (b)–(d) Visualized selected m/z species representing features to pars distalis (m/z 6,651; green), pars intermedia (m/z 2,897; red), and pars neuralis (m/z 9,685; yellow). (e) Merge of (a–d). (f) MALDI-TOF-MS spectra obtained from this case from pars distalis (green), pars intermedia (red), and pars neuralis (yellow) showing the molecular differences between the histological regions. Reprinted from Walch *et al.* (2008) with permission from Springer. (See Color Insert.)

and another section is cut for histological staining. They can then be superimposed on each other and provide an absolute value of the molecular distribution (Figure 5). Recently a new approach for tissue section staining after the MALDI measurement has been reported. The results obtained from IMS analysis were correlated with the H&E staining of the tissue section (Schwamborn *et al.*, 2007).

3.2. Choice of Matrix

The choice of a suitable matrix for MALDI-IMS analysis depends on the mass range and analyte of interest. The main function of the matrix is to absorb laser energy from the source and transfer it to the analyte (Dreisewerd, 2003). The matrix thus ensures that efficient desorption and ionization occur and protects the tissue section from the disruptive energy of the laser. Sinapinic acid is generally used for the analysis of higher-molecular-weight proteins, and α -cyano-4-hydroxycinnamic acid (CHCA) is used for lower-molecular-weight molecules such as peptides (Schwartz *et al.*, 2003). 2,4-dihydroxybenzoic acid (DHB) and 2,6-dihydroxyacetophenone (DHA) are generally used for analysis of

TABLE 1 Commonly used MALDI matrices for imaging of biomolecules in tissue samples

Matrix	Applications	References
2,5-Dihydroxybenzoic acid (DHB)	Lipids, Sugars, peptides, nucleotides, glycopeptides, glycoproteins, and small proteins	Fournier <i>et al.</i> (2003); Herring <i>et al.</i> (2007); Tholey and Heinzle (2006)
α -Cyano-4-hydroxycinnamic acid (CHCA)	Peptides, small proteins and glycopeptides	Schwartz <i>et al.</i> (2003); Tholey and Heinzle (2006)
2,6-Dihydroxyacetophenone (DHA)	Phospholipids	Jackson <i>et al.</i> (2005); Seeley <i>et al.</i> (2008); Tholey and Heinzle (2006)
2,4,6-Trihydroxyacetophenone (THAP)	Lipids	Stuebiger and Belgacem (2007)
<i>p</i> -nitroaniline (PNA)	Phospholipids	Estrada and Yappert (2004); Rujoi <i>et al.</i> (2004)
2-mercaptobenzothiazole (MBT)	Phospholipids	Astigarraga <i>et al.</i> (2008)
Sinapinic acid (SA)	Peptides and large proteins	Schwartz <i>et al.</i> (2003)
CHCA/aniline, ionic matrix	Peptides	Lemaire <i>et al.</i> (2006b)
CHCA/ <i>n</i> -butylamine, ionic matrix	Phospholipids	Shrivastava <i>et al.</i> (2010)

phospholipids (Herring *et al.*, 2007; Seeley *et al.*, 2008). A great variety of matrices are used for the analysis of biomolecules, some of which are listed in Table 1.

3.2.1. Ionic Matrices for IMS

Ionic matrices (IMs) constitute a new class of organic matrices reported for the analysis of a number of different molecules in MALDI-MS. IMs are good for MALDI-MS imaging studies due to the fact that the process solubilizes several analytes, has vacuum stability, and forms homogenous crystals with analyte molecules. IMs have been used to obtain enhanced sensitivity and good reproducibility in the analysis

of biomolecules (Armstrong *et al.*, 2001; Laremore *et al.*, 2007). IMs such as 2,5-dihydroxybenzoic acid butylamine (DHBB) and α -cyno-4-hydroxycinnamic acid butyl amine (CHCAB) render good crystal formation, signal intensity, and reproducibility compared with conventional matrices such as DHB and CHCA (Shrivastava *et al.*, 2010). The results are

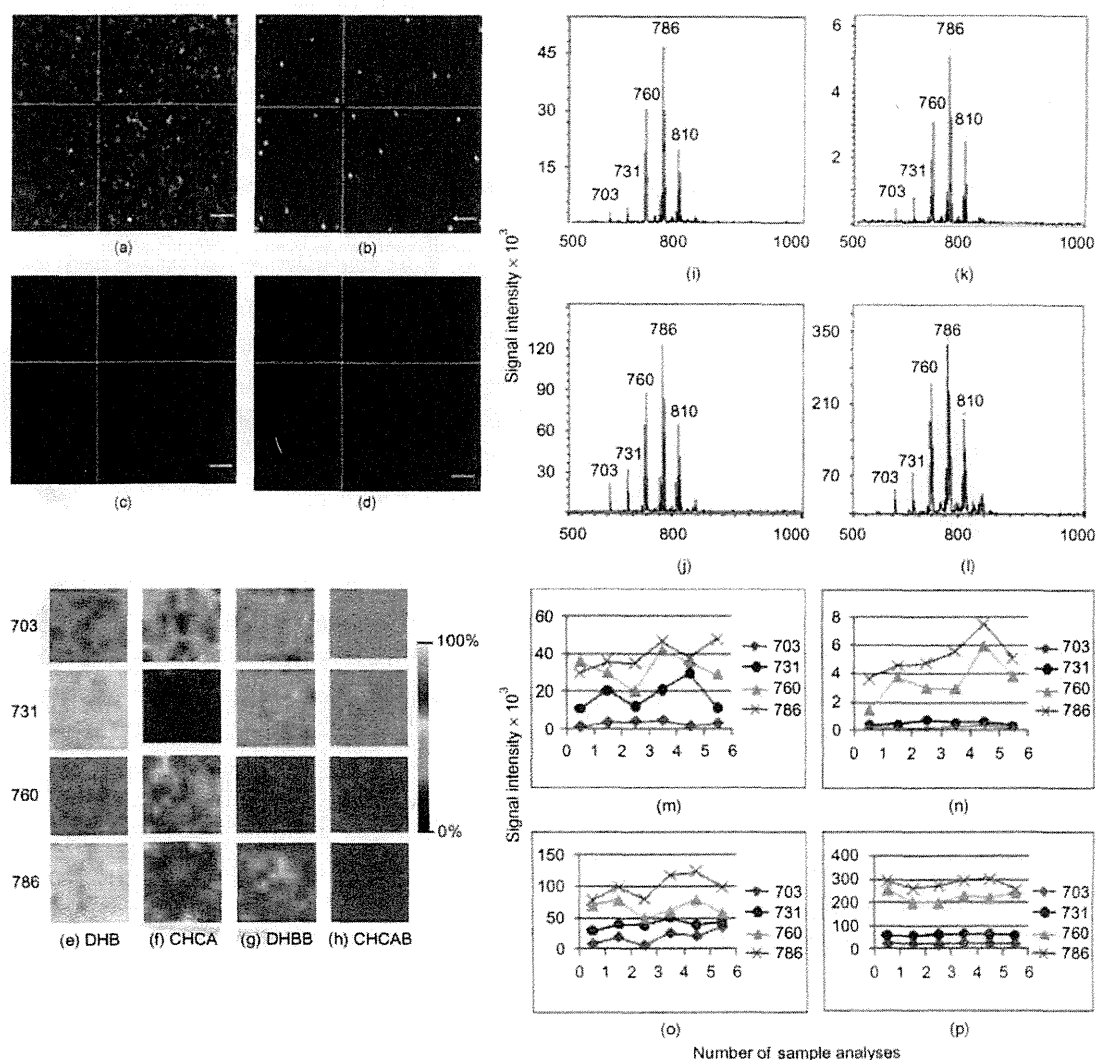


FIGURE 6 The crystal formation of (a) DHB, (b) CHCA, (c) DHBB, and (d) CHCAB matrixes with phospholipids on to a MALDI target plate. The pictures were taken with an Ultraflex II TOF/TOF. The scale bar (white color line) is 100 μm ; images (e) to (h) show the ion image of phospholipids reconstructed obtained by using (e) DHB, (f) CHCA, (g) DHBB, and (h) CHCAB matrix at m/z 703, 731, 760, and 786. Images (i) to (l) show the signal enhancement: 3- to 7-fold enhancement of signal intensity when DHBA IM (image i) is used as a matrix compared with DHB matrix (image j) and 50- to 100-fold improvement of signal intensity using CHCAB IM (image k) compared with CHCA matrix (image l). Graphs (m) to (p) show the six replicate analyses of samples with \pm relative standard deviation, % by using (m) DHB: \pm 20.5–40.8%, (n) CHCA: \pm 29.5–45.8%, (o) DHBB: \pm 14.5–21.8%, and (p) CHCAB: \pm 7.5–10.0%. Reprinted from Shrivastava *et al.* (2010) with permission from American Chemical Society. (See Color Insert.)

shown in Figure 6. Direct tissue analyses of peptides in rat brain tissue sections using IMs improved the ionization efficiency and increased the signal intensity of ion images of molecules compared with the conventional matrix (Lemaire *et al.*, 2006a). IMs were also used for imaging and identification of gangliosides in mouse brain (Chana *et al.*, 2009). DHB and CHCAB IMs in MALDI-IMS were also used for analysis of mouse liver and cerebellum tissues to identify the different species of lipids; results with CHCAB were better than with conventional matrices (DHB and CHCA).

3.2.2. Nanoparticles as Matrices for IMS

In addition, nanoparticles (NPs) can be used as a matrix instead of organic matrices for the analysis of low-molecular-weight molecules (< 500 Da). One problem with the organic matrix ions is that they themselves produce an intense peak in the mass spectrum and hence suppress detection of the analyte of interest, which then obviously decreases the sensitivity of the method. To circumvent this disadvantage, nanomaterials and inorganic compounds have been introduced. The Tanaka and Sunner groups investigated the application of cobalt powder (NPs) and graphite microparticles, respectively, suspended in glycerol to analyze proteins and/or peptides in MALDI-MS analyses. The use of NPs as a matrix in MALDI-MS allows for efficient absorption of laser energy as well as efficient subsequent desorption and ionization of molecules from the sample surface (Sunner *et al.*, 1995; Tanaka *et al.*, 1988). Desorption/ionization on porous silicon (DIOS) is another matrix-free method that is produced by etching of the silicon surface. Small molecules can be efficiently ionized using DIOS as an effective surface (Wei *et al.*, 1993). Today nanomaterial surfaces are also applied for the direct analysis of tissue samples in MALDI-IMS. Northen's group introduced a new nanostructure surface for imaging of biomolecules in tissue samples known as ionization nanostructure-initiator mass spectrometry (NIMS) (Northen *et al.*, 2007). Several other sample preparation procedures, such as graphite-assisted laser desorption/ionization (GALDI) (Cha and Yeung, 2007), nano-assisted laser desorption/ionization (NALDI) (Vidova *et al.*, 2010), and DIOS have been proposed for imaging of biomolecules in tissue samples. Taira *et al.* (2008) developed another matrix-free method called nanoparticle-assisted laser desorption/ionization imaging mass spectrometry (Nano-PALDI-IMS) that can be used to visualize peptides, phospholipids, and metabolites in tissue sections. Recently silver (Hayasaka *et al.*, 2010) and gold (Goto-Inoue *et al.*, 2010a) NPs were applied for imaging and identification of fatty acids and glycosphingolipids, respectively, an analysis that could be difficult to perform by conventional MALDI-MS using DHB as a matrix. Figure 7 demonstrates imaging and identification of fatty acids from mouse liver sections using silver NPs as a matrix (Hayasaka *et al.*, 2010). More recently, TiO₂ NPs were applied for the analysis of low-molecular

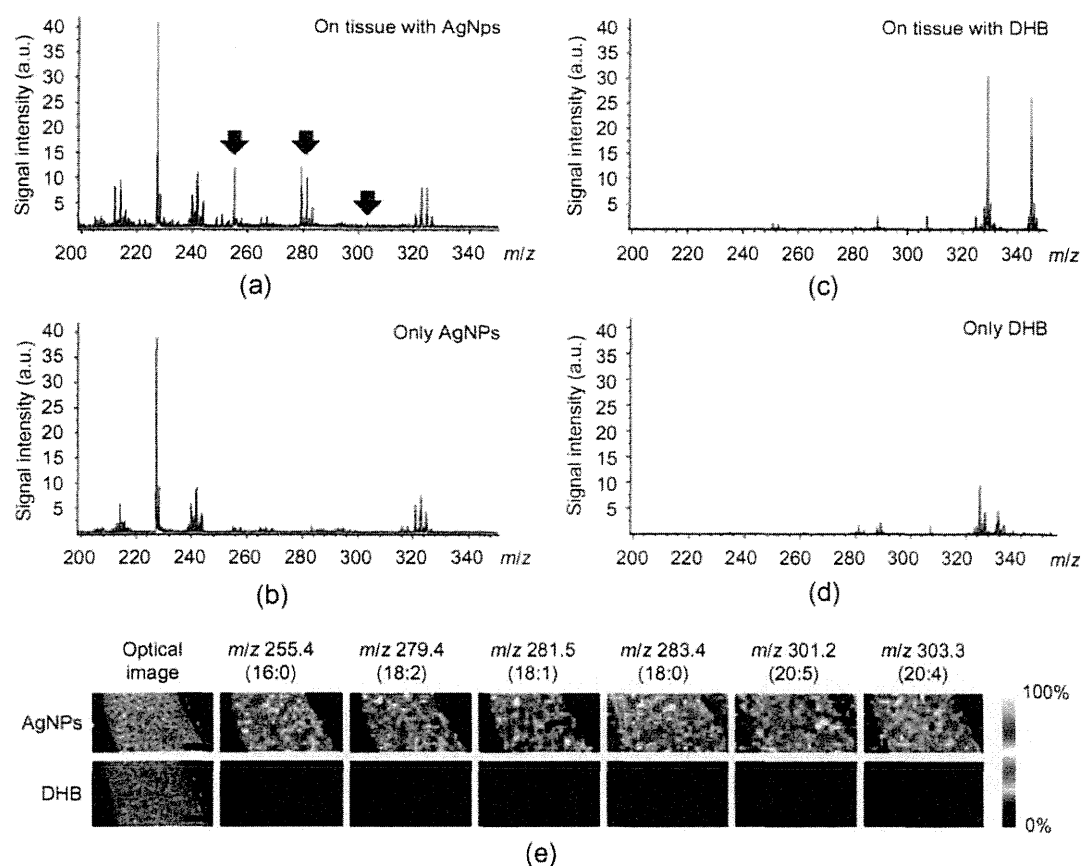


FIGURE 7 Identification of fatty acids from mouse liver sections in nano-PALDI-IMS. The serial sections were sliced to a thickness of 10 μm . Silver nanoparticles (NPs) or DHB matrix solution was sprayed on the surface of the mouse liver sections, respectively. Their sections were measured with a scan pitch of 100 μm by nano-PALDI-IMS analysis in negative-ion mode. The mass spectra were obtained from the sections sprayed with silver NPs (a) on tissue section, (b) only silver NPs or DHB matrix, (c) on tissue section, and (d) only DHB solution. The peaks used to reconstruct the ion image are indicated by arrows. (e) In the analysis using silver NPs and DHB, the ion signals at m/z 255.4 (16:0), 279.4 (18:2), 281.5 (18:1), 283.4 (18:0), 301.2 (20:5), and 303.3 (20:4) were detected. The scale bars are 500 μm . Reprinted from Hayasaka *et al.* (2010) with permission from Springer. (See Color Insert.)

weight-biomolecules in mouse brain without observing any NP-related peaks. More individual signals and higher intensity were obtained when TiO_2 NPs were used as a matrix compared with a DHB matrix (Shrivastava *et al.*, 2011). Thus we can conclude that the use of a nanomaterial surface is efficient and effective for desorption and ionization of molecules; the process yields images with higher resolution.

3.3. Application of Matrix Solution

The deposition of matrix solution on the surface of a tissue section is another important step in obtaining homogeneity, reproducibility, and good resolution of the biomolecule. The matrix solution consists of three

components—organic solvent, matrix, and trifluoroacetic acid (TFA). Crystal formation is affected by the concentration of matrix and the ratio of organic solvent to water; organic solvent is used to dissolve the solid matrix and extract the molecules from the tissue section. This extraction is followed by crystal formation on the surface of the tissue section. The addition of TFA provides free protons for effective ionization of the analytes, and typically, singly charged $[M + H]^+$ ions are formed. A number of devices are useful for the deposition of matrix solution on the surface of tissue sections—for example, chemical inkjet printer spotter (Baluya *et al.*, 2007), robotic spotting depositors (Aerni *et al.*, 2006), electro-spray depositors (Altelaar *et al.*, 2007), and airbrush sprayers (Hayasaka *et al.*, 2009). The sublimation (Hankin *et al.*, 2007) and stainless steel sieve (Puolitaival *et al.*, 2008) methods have demonstrated good signal intensity and sample reproducibility. Figure 8 shows a thin layer chromatography (TLC) sprayer (image a), sublimation apparatus (b), air brush sprayer (c), and a chemical inkjet printer (d) used for matrix deposition. The goal of these matrix deposition approaches is to improve the homogeneity of the sample surface and enhance the signal intensity for the identification of biomolecules compared with direct deposition of the matrix.

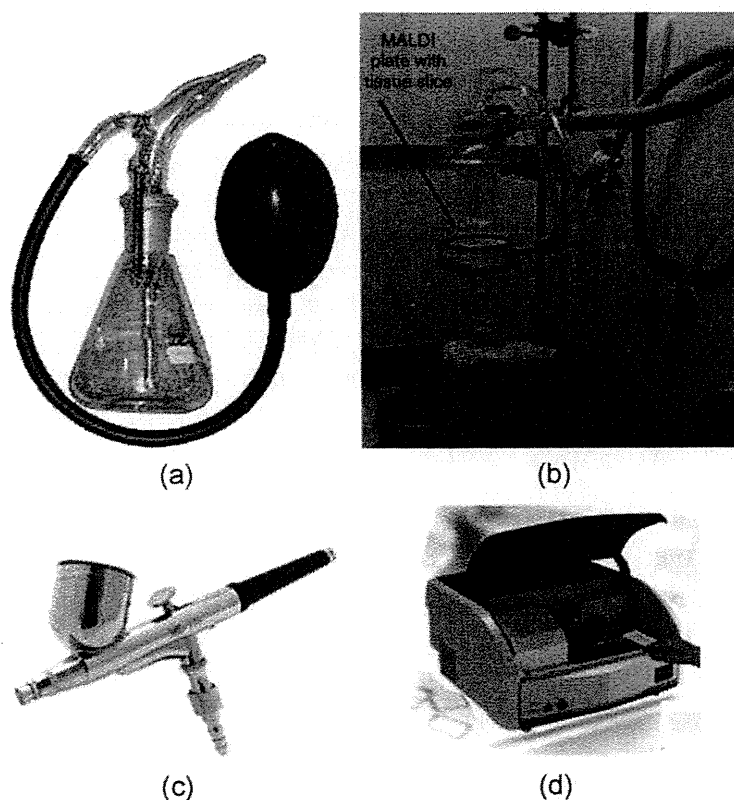


FIGURE 8 Apparatus used to deposit matrix on the tissue section. (a) Thin-layer chromatography sprayer, (b) sublimation apparatus, (c) air brush sprayer, and (d) chemical inkjet printer. Reprinted from Hankin *et al.* (2007) with permission from Springer.

4. INSTRUMENTATION

4.1. Quadrupole Mass Analyzer

A quadrupole mass analyzer is made from four parallel rods maintained at fixed direct current (DC) with an alternating radiofrequency (RF). With this setup molecular ions formed at the source pass through the middle of the quadrupoles in the electric field region and the ions of a specific m/z have a stable trajectory path and may pass all the way to the detector, while the remaining ions collide with the electrodes and never reach the detector (Gross, 2004). Using a continuous and controlled manner to change the frequency and potential, the quadrupole transmits molecules at certain m/z values. Figure 9a shows a diagram of quadrupole mass analyzer. The sensitivity of the instrument can be enhanced by increasing the number of quadrupoles from two to three (triple quadrupole) in series. In triple-quadrupole analyzers, the first (Q_1) and third (Q_3) quadrupoles act as filters, and the second (Q_2) quadrupole functions as a collision cell. The third (Q_3) quadrupole is worked at normal RF/DC or in the linear ion trap (LIT) mode (Douglas *et al.*, 2005). Hopfgartner *et al.* (2009) demonstrated the fast imaging of complete rat sections using MALDI coupled with a triple-quadrupole LIT where the precursor ion mode can be used to monitor the presence of the parent drug in the tissue section.

4.2. Time-of-Flight Mass Analyzer

The TOF-MS analyzer has become valuable for direct analysis of biomolecules from tissue samples. In TOF-MS, the different masses of ions are separated based on their differences in travel time through a drift region. The lighter ions produced from the source travel faster at the end of the drift region compared with heavier ions in the tube (see Figure 9b). However, TOF-MS has disadvantages in mass accuracy, resolving power, and its inability to perform tandem MS experiments (Goto-Inoue *et al.*, 2011; Gross, 2004). This drawback has been overcome by the introduction of an orthogonal geometry (oTOF)-MS analyzer to extract pulsed ions from a continuous ion beam. Huang *et al.* (2011) investigated the use of oTOF-MS for imaging and simultaneous detection of metal and nonmetal elements in tissue section with spatial resolution of 50 μm .

Ion mobility (IM) spectrometry can also be coupled with the TOF-MS system for direct analysis of tissue samples. The instrument has oTOF-MS and is equipped with an IM spectrometer located between the quadrupole and the TOF-MS analyzer. The IM spectrometer separates ions based on their IM (i.e., their shape) and TOF-MS separates ions according to their m/z ratio in the MS (Verbeck *et al.*, 2002). Separation of structurally similar

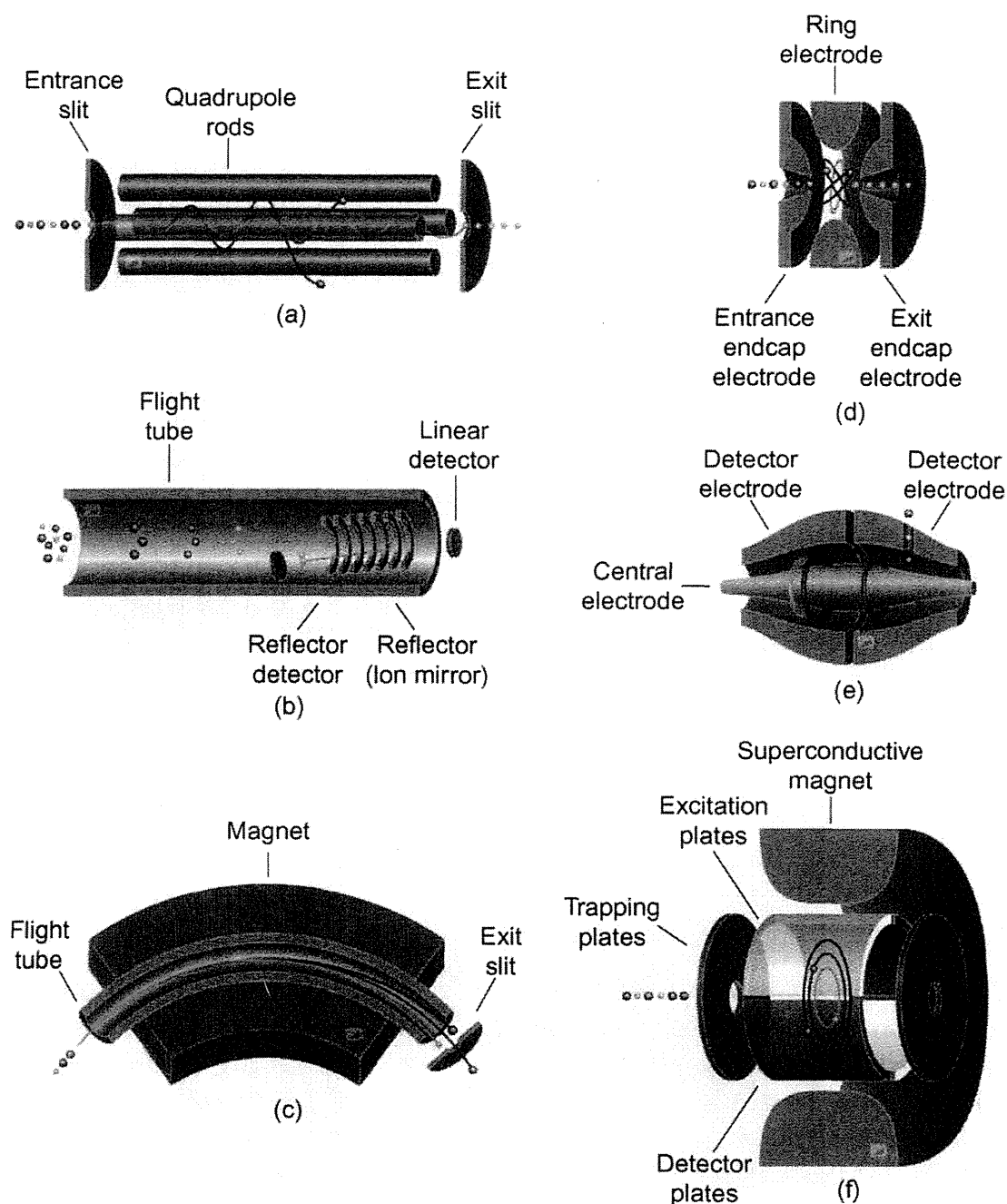


FIGURE 9 Schematic description of six mass analyzers used in mass spectrometers. (a) Quadrupole, (b) time-of-flight, (c) magnetic sector, (d) ion trap, (e) orbitrap, (f) ion cyclotron resonance. Reprinted from Pol *et al.* (2010) with permission from Springer. (See Color Insert.)

ions and ions of the same charge state is thus possible through their different mobility in the IM spectrometer. The combined techniques of IM and TOF-MS were used for imaging and identification of digested proteins. IM separates isobaric ions that cannot be distinguished by MALDI-TOF alone, providing mass- and time-selected ion images of biomolecules in tissue samples (Stauber *et al.*, 2010).

In addition, the combination of a quadrupole (Q) mass analyzer with a TOF-MS is called a Q-TOF-MS system and is used for structural analysis with tandem MS. The localization of a xenobiotic substance in skin has been reported by applying a Q-TOF-MS (Bunch *et al.*, 2004). Another approach for imaging and identification of molecules is the combination of two TOF mass analyzers; this hybrid is called TOF/TOF. First, TOF-MS separates precursor ions using a velocity filter; second, TOF-MS analyzes the fragment ions (Gross, 2004). MALDI-TOF/TOF is a simple, rapid, and sensitive technique for MALDI imaging of biomolecules in tissue sections (Hayasaka *et al.*, 2010; Sugiura *et al.*, 2009).

4.3. Sector-Type Mass Analyzer

The sector mass spectrometer consists of large electromagnetic ("B" sector) and electrostatic focusing devices ("E" sector) that, depending on the different manufacturers' use, differ in their geometries (Cottrell and Greathead, 1986). The motion of the ions in the trajectory pathway depends on the strength of electric and magnetic field where each ion (m/z) travels with different speeds (see Figure 9c). Magnetic sectors are used for high-resolution elemental imaging and identification of samples in combination with dynamic SIMS. The magnetic sector and several movable detectors allow a simultaneous detection of several elements or small molecules (within a narrow mass range) with higher sensitivity. Slodzian *et al.* (1992) used a SIMS coupled with a magnetic sector double-focusing mass spectrometer for simultaneous imaging of several elements in tissue sample.

4.4. Ion Trap Mass Analyzer

A quadrupole ion trap (QIT or 3D-IT) operates in a 3D quadrupole field maintained at constant DC and RF fields to trap the moving ions of m/z range. A QIT consists of three hyperbolic-shaped electrodes: the central ring electrode and two adjacent end cap electrodes (entrance and exit) (see Figure 9d). A 3D-IT is a small, relatively inexpensive instrument for sensitive analysis; it can also be used for MS^n analysis of molecules in the tissue samples (Gross, 2004; Hopfgartner *et al.*, 2004). Shimma *et al.* (2008) reported their use of a MALDI-QIT-TOF-MS instrument for imaging of phospholipids, glycolipids, and tryptic-digested proteins. MS analyses were performed to confirm their presence. Recently a mass microscope coupled with a high-resolution atmospheric pressure-laser desorption/ionization (AP-MALDI) and QIT-TOF was used for imaging and identification of volatile substances in ginger (Harada *et al.*, 2009). This instrument allows researchers to precisely determine the

specific tissue section prior to IMS and has spatial resolution ($10\ \mu\text{m}$) higher than the naked eye.

In a linear quadrupole ion trap (LIT) or 2D traps (2D-IT), the ions are trapped in a 2D quadrupole field and then pass axially. The 2D-IT ion trap produces reasonable mass accuracy, mass resolution, and sensitivity (Schwartz *et al.*, 2002). LIT has a better ion storage capacity and a higher trapping efficiency compared with 3D-IT. However, the disadvantage of LIT is the relatively narrow mass range of small molecule analysis. Garrett *et al.* (2007) described a new MALDI-LIT-MS for imaging of tissue samples and also used for MS^n analyses to confirm the molecules. Enomoto *et al.* (2011) demonstrated the visualization of phosphatidylcholine (PC), lysophosphatidylcholine, and sphingomyelin in mouse tongue using LTQ (linear trap quadrupole)-MALDI-IMS (Enomoto *et al.*, 2011).

4.5. Orbitrap Mass Analyzer

In an orbitrap mass analyzer, the ions are rotated around a central electrode by applying an appropriate voltage between the outer and central electrodes. Hence, the ions of a specific m/z ratio cycle in rings that oscillate around the central spindle and then pass through the detector (Makarov *et al.*, 2006). Figure 9e shows the overview of the orbitrap mass analyzer. LTQ-Orbitrap has been used to analyze compounds with high resolving power and excellent mass accuracy that appreciably decrease false-positive peptide identifications in the sample (Adachi *et al.*, 2006; Makarov *et al.*, 2006). Verhaert *et al.* (2010) demonstrated the use of LTQ-orbitrap for imaging of neuropeptides in neural tissue samples. In addition, it has also been used for identification and sequencing of neuropeptides from neural tissue using MALDI-MS with an ion trap-orbitrap hybrid instrument. Landgraf *et al.* (2009) showed the high resolution and accurate measurement of ion images of lipids in spinal cord using MALDI-LIT-orbitrap-MS. Manicke *et al.* (2010) demonstrated imaging of lipids in rat brain tissue section with a high-resolving power instrument of DESI-LTQ-orbitrap-MS.

4.6. Ion Cyclotron Resonance Mass Analyzer

In an ion cyclotron resonance (ICR)-MS analyzer, the ions of a particular m/z ratio are isolated based on the cyclotron frequency of the ions in a constant magnetic field. The oscillation of ions in ICR induces an alternating current that is equivalent to their m/z ratios. Figure 9f shows the schematic for an ICR analyzer. Fourier transforms (FT)-ICR-MS continues to deliver the highest mass-resolving power and mass measurement accuracy (Gross, 2004). The combination of MALDI-TOF-MS with the FT-ICR-MS technique is useful for high-spatial resolution analysis and

identification of unknown biomolecules in tissue samples. Thus the high mass resolution of the FT-ICR-MS can be used to analyze compounds that cannot be distinguished with lower-mass resolution mass spectrometers (Taban *et al.*, 2007; Wang *et al.*, 2011). MALDI-FT-ICR has also been reported for IMS analysis of drugs and metabolites in tissue. The accurate mass measurement can be performed using FT-ICR-MS, which provided a molecular specificity for the ion images obtained from tissue sample analysis (Cornett *et al.*, 2008).

5. IMS MEASUREMENTS

MALDI-IMS experiments can be performed after the deposition of matrix on the tissue section and using different types of MS instruments as discussed above. The setting of the laser energy, detector gain, and random walk function are optimized in order to obtain better signal intensity of the target molecules during the IMS analysis. Either a particular region of the tissue or the entire tissue section is selected for analysis, depending on the particular interest. At present, the commercially available instruments can perform IMS analyses with the highest spatial resolution of $\sim 25 \mu\text{m}$ (Goto-Inoue *et al.*, 2009a). Recently we developed a mass microscope that can move a sample stage by $1 \mu\text{m}$, and the finest size of the laser diameter is approximately $10 \mu\text{m}$ (Harada *et al.*, 2009). The measurement time of IMS experiments depends on the number data spots, the frequency of the laser, and the number of shots per spot.

6. DATA ANALYSIS

Due to the large (gigabytes) size of the dataset, high-capacity visualization software is required to visualize the ion image and distribution pattern of biomolecules in tissue samples. New computing methods are required for both rapid, accurate data acquisition and the interpretation of the IMS analysis results. Therefore, in addition to instrumental improvements, data acquisition and software development have been important for the production of reliable data. The databases used are based on algorithms that perform analysis through statistical evaluation of observed and theoretical spectra of biomolecules. BioMap (<http://www.maldi-msi.org>, Novartis, Basel, Switzerland) and flexImaging (<http://www.bdal.com>, Bruker Daltonics GmbH, Bremen, Germany) imaging software are used to identify biomolecules in various sample types. The intensity of the different color images obtained by both software packages can relate the distribution of biomolecules in the tissue section. These software packages also help in understanding the localization of biomolecules at

particular regions of interest (ROIs) for mass spectral comparison and other statistical analysis.

BioMap imaging software can be used for different instruments such as PET, nuclear magnetic resonance (NMR), computed tomography (CT), and near-infrared fluorescence (NIRF) as the result of multiple modifications. Interactive data language Virtual Machine (Research Systems, Boulder, CO) is required in the system to process the data obtained from IMS analysis. BioMap software can also be used for baseline correction, spatial filtering, and averaging of spectra for presentation of the IMS results.

The flexImaging software is used for the acquisition and evaluation of MALDI-TOF imaging results. The mass peaks (at m/z) obtained in the mass spectrum are normalized to total ion current and then the peak intensity is taken into account to study the molecules distribution on the tissue section. The imaging MS experiments are performed by collecting spectra at a resolution of 50 to 400 μm in the same m/z range as above. Principal component analysis (PCA) is an unsupervised statistical method used to identify groups of closely correlated variables; for MS imaging datasets these variables are spatial coordinates and mass. This approach also reduces the multidimensional datasets to the lower dimensions (Chou, 1975). PCA analysis is performed using ClinProTools 2.1 software (Bruker Daltonics). Zaima *et al.* (2009) performed a PCA for screening of metabolites in the fatty liver. Several differences were found in identifying the metabolites in fatty and normal liver tissue samples. PCA was also used in proteomics studies (Deininger *et al.*, 2008; Djidja *et al.*, 2010; Yao *et al.*, 2008).

7. APPLICATIONS OF IMS FOR DIRECT ANALYSIS OF TISSUE

7.1. IMS for Lipidomics

Lipids are the main constituents of cell membranes; the major functions of lipids are transportation of ions and signals across the cell membrane. Various types of lipids, such as glycerophospholipids (GPLs), sphingolipids, sterol lipids, saccharolipids, waxes, and fat-soluble vitamins are found in biological systems. Membranes act as barriers to separate compartments within eukaryotic cells and to separate all cells from their surroundings (Brown, 2007; Fahy *et al.*, 2009; Lee *et al.*, 2003). The identification and quantification of lipids in tissue sample can help in understanding several biosynthetic and metabolic pathways that govern human diseases, such as insulin-resistant diabetes, Alzheimer's disease, schizophrenia, cancer, atherosclerosis, and infectious diseases (Oresic *et al.*, 2008). Thus the analysis of lipids in tissue samples is a very important issue. High-performance liquid chromatography (HPLC) (McCluer *et al.*, 1986), TLC (Touchstone,

1995), and MS have been used to analyze lipids in tissue samples. However, the sample preparation procedures in chromatographic techniques are lengthy and the localization of biomolecules in tissue sample surface cannot be established. Therefore, different IMS systems are successfully used for imaging of lipids. The analysis of glycerophospholipids, sphingolipids, and neutral lipids is discussed in detail in the following sections.

7.1.1. Glycerophospholipids

GPLs are glycerol-based phospholipids and essential components of cell membranes. They act as second messengers involved in cell proliferation, apoptosis, and metabolism. The determination of GPL content in tissue samples is useful for finding potential biomarkers for diseases such as atherosclerosis or rheumatism (Fuchs *et al.*, 2005; Schmitz and Ruebsaamen, 2010). Altered levels of lipids are found in many pathological conditions such as Alzheimer's disease (Han *et al.*, 2001, 2002), Down syndrome (Murphy *et al.*, 2000), diabetes (Han *et al.*, 2007), and Niemann–Pick disease (He *et al.*, 2002). Figure 10 illustrates the basic structures of common classes of GPLs such as PC, phosphatidylethanolamine (PE), phosphatidylinositol (PI), and phosphatidylserine (PS) (Jackson and Woods, 2009). PC is easily ionized due to its charged quaternary ammonium head group and has thus become a popular lipid species to investigate (Pulfer and Murphy, 2003). The ionized molecules observed in the mass spectrum are usually either protonated $[M+H]^+$, sodiated $[M+Na]^+$, or potassiumated $[M+K]^+$ in positive-ion mode. Phospholipids such as PE, PS, PA, PG, and PI may generate negative ions due to the presence of the phosphodiester moiety and display molecular anions $[M-H]^-$ (Fuchs *et al.*, 2010). The addition of potassium acetate (Sugiura *et al.*, 2009) or LiCl (Jackson *et al.*,

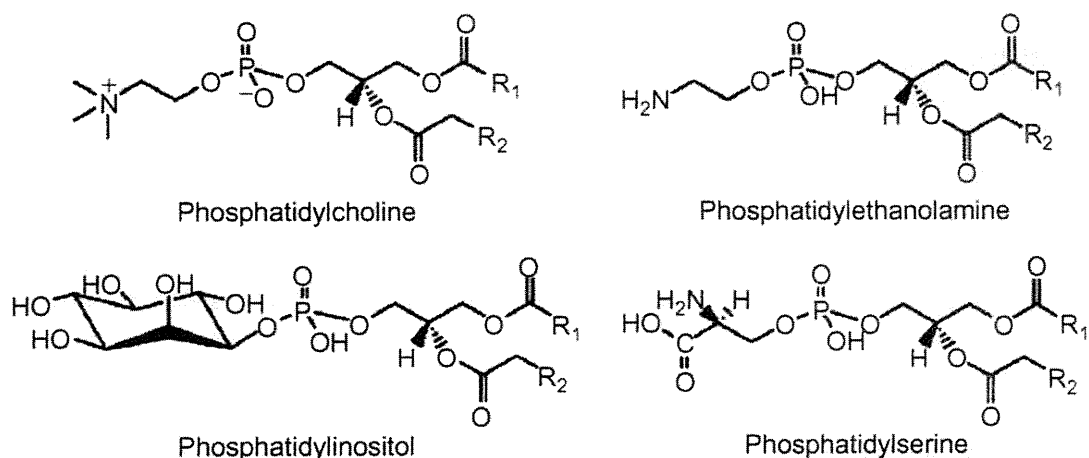


FIGURE 10 Structure of glycerophospholipids. Reprinted from Jackson and Woods (2009) with permission from Elsevier Science.

2005) to the matrix solution has also been reported for effective ionization of molecules in tissue samples.

The selection of MALDI matrices is an important issue. For MALDI-IMS, the matrix should have good vacuum stability and homogenous crystal formation containing analyte molecules. Various matrices have been reported for the identification and characterization of lipids in MALDI-MS, including DHB (Petkovic *et al.*, 2001; Puolitaival *et al.*, 2008; Schiller *et al.*, 1999), DHA (Jackson *et al.*, 2005; Shimma *et al.*, 2007), p-nitroaniline (PNA) (Estrada and Yappert, 2004; Rujoi *et al.*, 2004), and 9-aminoacridine (Eibisch and Schiller, 2011; Teuber *et al.*, 2010). However, PNA and dihydroxyacetone phosphate (DHAP) were unstable under high vacuum conditions and started to evaporate after their introduction into the MALDI-MS instrument (Jackson *et al.*, 2005; Rujoi *et al.*, 2004; Shrivastava *et al.*, 2010). DHB matrix exhibited a lower sensitivity for the detection of PA, PS, PE, PI, and PG in negative-ion mode, possibly due to its acidity (Estrada and Yappert, 2004; Petkovic *et al.*, 2001). DHA can be used in both positive and negative ionization modes for analysis of phospholipids (Woods *et al.*, 2006). PNA is another good matrix for the analysis of phospholipids in either positive-ion or negative-ion modes (Estrada and Yappert, 2004). Recently, 2-mercaptobenzothiazole (MCT) was added as an alternative to the use of DHB for MALDI-MS analysis of phospholipids in brain and liver tissue samples (Astigarraga *et al.*, 2008). The main advantages of MCT over the commonly used matrices DHB, DHA, and PNA are low vapor pressure, low acidity, and homogenous crystal formation, which allowed for detection of more lipid species in negative mode, with high sensitivity and high detection reproducibility. Ionic matrices have also been used in MALDI-IMS owing to the good vacuum stability, homogenous crystal formation, and good solubility of analytes for efficient ionization and desorption of molecules (Chana *et al.*, 2009; Lemaire *et al.*, 2006a; Shrivastava *et al.*, 2010). Shrivastava *et al.* (2010) used an ionic matrix of CHCAB to image and identify lipids in mouse cerebellum and found that this ionic matrix yields a higher number of ion images compared with the use of DHB matrix in MALDI-IMS (Figure 11). Use of NPs is another good approach for selective and sensitive analysis of lipids and small metabolites in tissue samples without matrix-oriented peaks in the low-molecular-mass range (Cha and Yeung, 2007; Goto-Inoue *et al.*, 2010a; Hayasaka *et al.*, 2010; Shrivastava *et al.*, 2011; Taira *et al.*, 2008).

Sugiura *et al.* (2009) showed the imaging of polyunsaturated fatty acid-containing PC in mouse brain using MALDI-IMS. The results demonstrated that arachidonic acid (AA) and DHA-containing PC were found in the hippocampal neurons and cerebellar Purkinje cells, respectively. Figure 12 shows the localization of PC species in different layers of the mouse brain (Sugiura *et al.*, 2009). The distribution of PC species also has been reported in the mouse retinal section via MALDI-IMS analysis. The localization of PC (16:0/18:1) was found in the inner nuclear layer and

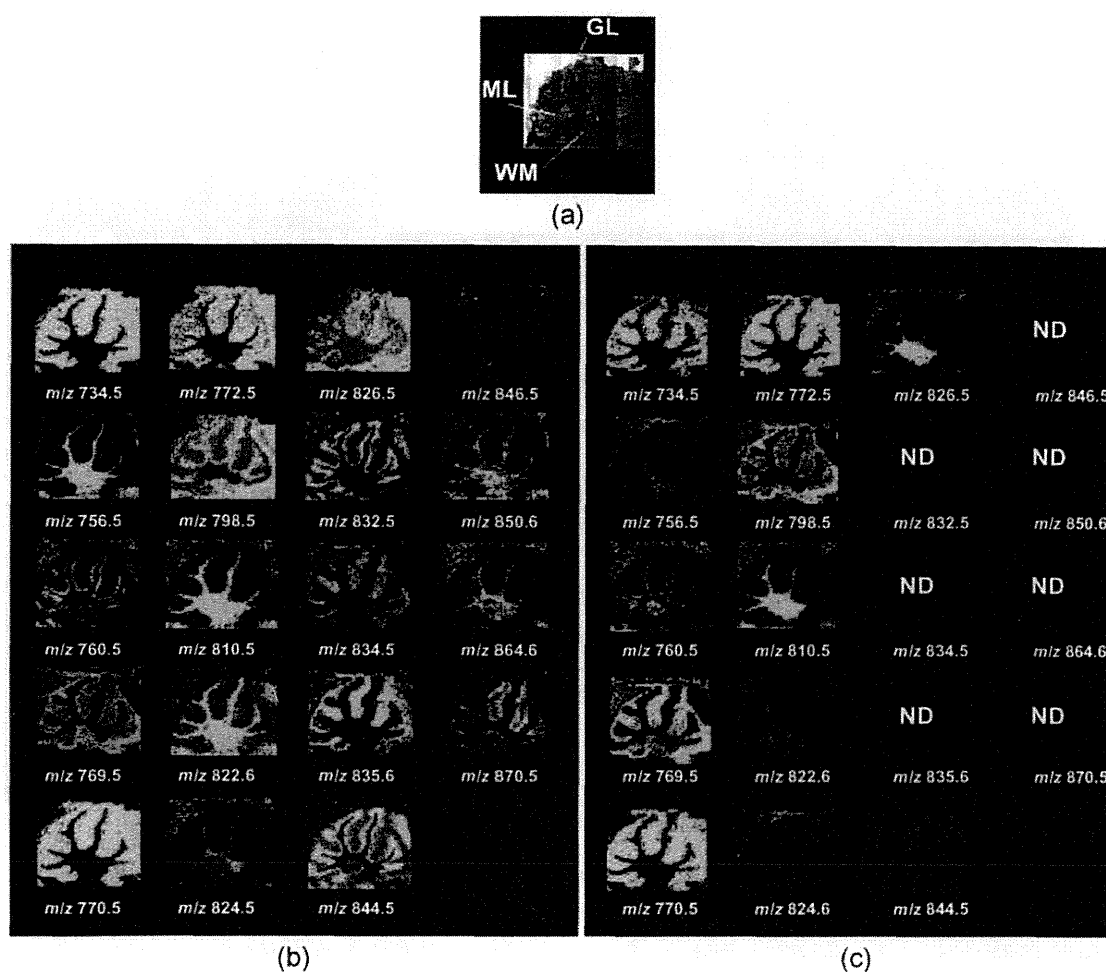


FIGURE 11 (a) H&E-stained mouse cerebellum showing three layers with 1.5-mm scale bar (white color). The ion images of lipids in mouse cerebellum tissue section obtained by using (b) CHCAB and (c) DHB as a matrix at m/z 734.5 $[(\text{PC}(16:0/16:0)+\text{H})]^+$, 770.5 $[\text{PC}(16:0/16:1)+\text{K}]^+$, 772.5 $[\text{PC}(16:0/16:0)+\text{K}]^+$, 798.5 $[\text{PC}(16:0/18:1)+\text{K}]^+$, 834.5 $[\text{PC}(18:0/22:6)+\text{H}]^+$, and 870.5 $[\text{PC}(18:1/22:6)+\text{K}]^+$ were localized in the molecular layer of cerebellum; at m/z 760.5 $[\text{PC}(16:0/18:1)+\text{H}]^+$, 832.5 $[\text{PC}(18:0/20:4)+\text{Na}]^+$, 844.5 $[\text{PC}(16:0/22:6)+\text{K}]^+$, and 846.5 $[\text{PC}(18:1/20:4)+\text{K}]^+$ were specific to the granular layer; and at m/z 756.5 $[\text{PC}(16:0/16:0)+\text{Na}]^+$, 810.5 $[\text{PC}(18:0/18:1)+\text{Na}]^+$, 824.5 $[\text{PC}(18:0/18:2)+\text{K}]^+$, and 826.5 $[\text{PC}(18:0/18:1)+\text{K}]^+$ and were found to be concentrated in the white matter of cerebellum. The ion images at m/z 769.5 $[\text{SM}(d18:1/18:0)+\text{K}]^+$ and 835.6 $[\text{SM}(d18:1/24:1)+\text{Na}]^+$ illustrated that the molecules were distributed in the region of molecular layer of tissue. The ion images at m/z 822.6 $[\text{GalCer}(d18:1/22:0)+\text{K}]^+$ and 850.6 $[\text{GalCer}(d18:1/24:0)+\text{K}]^+$ were localized in the white matter of mouse cerebellum. ND indicates the molecules were not detected. GL, granular layer; ML, molecular layer; WM, white matter. Reprinted from Shrivastava *et al.* (2010) with permission from American Chemical Society. (See Color Insert.)

the outer plexiform layer; PC (16:0/16:0) in the outer nuclear layer and inner segment; and PC (16:0/22:6) and PC (18:0/22:6) in the outer segment and pigment epithelium (Hayasaka *et al.*, 2008). Differential localization of PC (16:0/20:4) species was observed between terminal and stem villi of